2023 45th Annual International Conference of the IEEE Engineering in Medicine & Biology Society (EMBC) | 979-8-3503-2447-1/23/$31.00 ©2023 IEEE | DOI: 10.1109/EMBC40787.2023.10340455

Identification of Diabetic Small-Fiber Neuropathy Based on Electrophysiological and Psychophysical Responses to Intra-Epidermal Electric Stimulation using a Naïve Bayes Classifier

Boudewijn van den Berg†, Tom Berfelo†, Silvano R. Gefferie, Imre P. Krabbenbos, Jan R. Buitenweg

***Abstract*—Diagnosis and stratification of small-fiber neuropathy patients is difficult due to a lack of methods that are both sensitive and specific. Our lab recently developed a method to accurately measure psychophysical and electrophysiological responses to intra-epidermal electric stimulation, specifically targeting small nerve fibers in the skin. In this work, we study whether using one or a combination of psychophysical and electrophysiological outcome measures can be used to identify diabetic small-fiber neuropathy. It was found that classification of small-fiber neuropathy based on psychophysical and electrophysiological responses to intra-epidermal electric stimulation could match or even outperform current state-of-the-art methods for the diagnosis of small-fiber neuropathy.**

***Clinical Relevance*—Neuropathy is damage or dysfunction of nerves in the skin, often leading to the development of chronic pain. Small-fiber neuropathy is the most prevalent type of neuropathy and occurs frequently in patients with diabetes mellitus, but can also occur in other diseases or in response to chemotherapy. Early detection of neuropathy could help diabetic patients to adapt glucose management, and doctors to adjust treatment strategies to prevent nerve loss and chronic pain, but is impeded by a lack of clinical tools to monitor small nerve fiber function.**

I. Introduction

Clinical identification of small-fiber neuropathy and subsequent development of neuropathic pain is hampered by the lack of proper tools. Currently used nerve conduction tests target large sensory and motor nerves which are only affected in advanced neuropathy and insensitive to the loss of small intra-epidermal nerve fibers [1]. A number of methods that aim to measure quantity or function of small intra-epidermal nerve fibers is available including skin biopsy, thermal quantitative sensory testing, quantitative sweat measurement, laser evoked potentials, electrochemical skin conductance and autonomic cardiovascular tests, of which some achieve a high specificity (ranging from 0.39 to 0.96) but only a poor to moderate sensitivity (0.15 to 0.72) [2]. In addition, nociceptive processing changes as a result of the lost function in small nerve fibers, leading to neuropathic pain. Until today, no physiologic tests have been developed to monitor the subsequent development of neuropathic pain. The urge for new clinically applicable technologies sensitive to several phenotypes of small fiber neuropathy and the underlying mechanisms leading to neuropathic pain is widely expressed in literature, e.g. [3].

Recently, we developed a novel method for simultaneous psychophysical and neurophysiological testing of the human nociceptive function. This method uses an adaptive sequence of intra-epidermal electric stimuli (IES) to selectively activate small fibers in the skin (Aδ nociceptive fibers) and measures stimulus detection behavior and evoked brain responses from single and multi-pulse stimuli of various amplitudes (Fig. 1). Analysis of a rich collection of stimulus-response pairs into nociceptive detection thresholds (NDT) and brain evoked potentials (EP), permits identification of the functional properties of small epidermal nerve fibers and central nociceptive processing [4]. In healthy subjects, this NDT-EP method successfully quantifies the increase in various evoked potential components and detection probability caused by an increase of the stimulus amplitude or the temporal summation of multiple pulses [5]. We recently used the NDT-EP method to assess the sensitivity of these features to the effects of small-fiber neuropathy. Preliminary results suggest that patients with diabetic small-fiber neuropathy have a significantly higher detection threshold, lower detection reliability (i.e., psychometric slope), lower amplitude of the N1 in the evoked potential as well as a lower signal-to-noise ratio of the P2 and a lower standard deviation of the P2 in the evoked potential. In patients with small-fiber neuropathy, the detection threshold for nociceptive stimuli is higher due to a decreased amount of small-fiber afferents in the skin, while the latencies of peaks in evoked brain activity (N1 and P2) are shifted due to collateral activation of tactile afferents.

As a next step, we want to know whether we could use individual NDT-EP method outcomes to observe nerve loss in individual patients suffering from diabetic small-fiber neuropathy. The ultimate goal of a new method would be to achieve an earlier and better diagnostic performance than any other quantitative sensory testing method for small-fiber neuropathy. To explore whether NDT-EP method outcomes could improve diagnostic performance, we used minimum-redundancy maximum relevance feature selection to select the most important psychophysical and EEG features for identification of small-fiber neuropathy. We tested whether identification of small-fiber neuropathy can be improved by combining a subset of these features for naïve bayes classification of diabetic small-fiber neuropathy.

†The first two authors contributed equally to this work.

*Research supported by the Netherlands Organization for Scientific Research (NWO) and the Anesthesiology R&D department of the St. Antonius Hospital Nieuwegein, the Netherlands.

B. van den Berg, T. Berfelo, and J.R. Buitenweg are with the department of Biomedical Signals and Systems, Technical Medical Centre, University of Twente, Enschede, the Netherlands (e-mail: b.van.den.berg@utwente.nl).

I. P. Krabbenbos is with the Department of Anesthesiology, Intensive Care and Pain Medicine, St. Antonius Hospital, Nieuwegein, the Netherlands.

II. METHOD

The experiments presented in this paper (Sections II. A. – II. E.) used the same procedures that were also described in [4-6]. Machine learning methods were specifically selected for the high-dimensional feature set in the current application and described in Section II. F. All experimental procedures were approved by the local Medical research Ethics Committees United (MEC-U, file number: NL66136.100.18).

A. Participants

Psychophysical and evoked brain activity features were extracted from a larger dataset of 13 diabetes mellitus patients diagnosed with chronic painful peripheral neuropathy (DMp; 11 males; median age: 68.0), 20 pain-free patients diagnosed with diabetes mellitus (DM, 9 males, median age: 58.5 years) and 20 pain-free healthy controls (HC; 8 males, median age: 38.9 years) measured at the St. Antonius Hospital in Nieuwegein, the Netherlands.

B. Procedure

Participants were seated in a comfortable chair and instructed to focus their gaze at a fixed point on the wall. Intra-epidermal electric stimuli were applied to the back of the hand via a custom made electrode with 5 microneedles and centered around the detection threshold using an adaptive psychophysical procedure [5, 7]. Participants were instructed to release a response button whenever they detected a stimulus. Each stimulus was randomly chosen from an equidistant vector of 5 amplitudes. When a stimulus was reported as detected, all amplitudes were decreased by 0.025 mA. When a stimulus remained undetected, all amplitudes were increased by 0.025 mA. A total of 450 stimuli were continuously applied (Fig. 1). The total procedure had a duration of approximately 30 minutes (including familiarization test) per measurement, and was repeated on the contralateral hand.

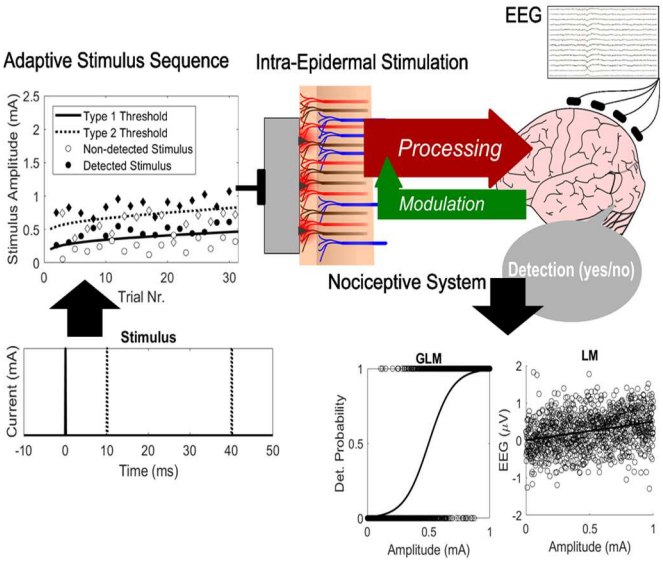

Figure 1. Simultaneous measurement of the nociceptive detection threshold (NDT) and evoked potential (EP), referred to as the NDT-EP method. In this method, the detection probability and threshold of multiple stimulus types (here with one or two pulses, 10 or 40 ms inter-pulse interval) is tracked using an adaptive algorithm while recording EEG. The effect of stimulus properties on the detection probability is quantified using a generalized linear model (GLM) and on the EEG using a linear model (LM). Reprinted with permission from [5].

D. Psychophysical Features

The 450 stimulus-response pairs obtained during each measurement were used to compute an average detection rate (R_{det}), average response time (RT_{mn}) and the standard deviation of the response time (RT_{std}). The generalized linear model in (1) (in Wilkinson notation) was fit to the stimulus-response pairs to compute effects of stimulus properties on the detection probability (P). The model quantified the effects of amplitude of the first pulse ($PU1$), amplitude of a second pulse with 10 ms inter-pulse interval ($PU2_{10}$), amplitude of a second pulse with 40 ms inter-pulse interval ($PU2_{40}$), trial number (TRL), and a model intercept on the log-odds of stimulus detection. Subsequently, model coefficients were used to compute the average detection thresholds and slopes of single-pulse and double-pulse stimuli with inter-pulse intervals of 10 and 40 ms (T_{SP}, T_{DP10}, T_{DP40}, S_{SP}, S_{DP10} and S_{DP40}).

$$\ln\left(\frac{P}{1-P}\right) \sim 1 + PU1 + PU2_{10} + PU2_{40} + TRL \quad (1)$$

E. Brain Activity Features

The EEG was recorded at 1000 Hz using a 64-channel Ag/AgCl electrode cap (10-20 system) during the entire experiment. The signal was divided into epochs -0.5 to 1.0 s with respect to stimulus onset and bandpass filtered between 0.1 and 40 Hz using the Fieldtrip toolbox in Matlab. Latencies of the N1 and P2 component of the evoked potential were estimated to be 190 and 440 ms respectively based on the grand average global field power. At both latencies the average and standard deviation of the evoked potential for each stimulus type and overall were computed. The linear model in (2) (in Wilkinson notation) was fit at both latencies to compute the effects of stimulus properties on the evoked potential (U_{EEG}). The model quantified the effects of amplitude of the first pulse ($PU1$), amplitude of a second pulse with 10 ms inter-pulse interval ($PU2_{10}$), amplitude of a second pulse with 40 ms inter-pulse interval ($PU2_{40}$), trial number (TRL), stimulus detection (D) and a model intercept on the evoked potential amplitude.

$$U_{EEG} \sim 1 + PU1 + PU2_{10} + PU2_{40} + TRL * D \quad (2)$$

TABLE I. ALL FEATURES USED FOR CLASSIFICATION AND THEIR CATEGORY. NOTE THAT SOME PSYCHOPHYSICAL FEATURES WERE COMPUTED USING THE GENERALIZED LINEAR MODEL (GLM) IN SECTION II.D., AND SOME BRAIN ACTIVITY FEATURES WERE COMPUTED USING THE LINEAR MODEL (LM) IN SECTION II.E.

Nr	Feature	Category
1	detection rate	psychophysics
2	response time: mean	psychophysics
3	response time: standard deviation	psychophysics
4	GLM: intercept	psychophysics
5	GLM: pulse 1	psychophysics
6	GLM: pulse 2, 10ms IPI	psychophysics
7	GLM: pulse 2, 40ms IPI	psychophysics
8	GLM: trial number	psychophysics
9	detection threshold: single-pulse	psychophysics
10	detection threshold: double-pulse, 10ms IPI	psychophysics
11	detection threshold: double-pulse, 40ms IPI	psychophysics
12	psychometric slope: single-pulse	psychophysics
13	psychometric slope: double-pulse, 10ms IPI	psychophysics
14	psychometric slope: double-pulse, 40ms IPI	psychophysics
15	LM of N1: intercept	brain activity
16	LM of N1: pulse 1	brain activity

17	LM of N1: pulse 2, 10ms IPI	brain activity
18	LM of N1: pulse 2, 40ms IPI	brain activity
19	LM of N1: trial number	brain activity
20	LM of N1: detection	brain activity
21	LM of N1: detection x trial number	brain activity
22	mean N1: all stimuli	brain activity
23	mean N1: single-pulse	brain activity
24	mean N1: double-pulse, 10ms IPI	brain activity
25	mean N1: double-pulse, 40ms IPI	brain activity
26	standard deviation N1: all stimuli	brain activity
27	standard deviation N1: single-pulse	brain activity
28	standard deviation N1: double-pulse, 10ms IPI	brain activity
29	standard deviation N1: double-pulse, 40ms IPI	brain activity
30	latency N1: all stimuli	brain activity
31	latency N1: single-pulse	brain activity
32	latency N1: double-pulse, 10ms IPI	brain activity
33	latency N1: double-pulse, 40ms IPI	brain activity
34	LM of P2: intercept	brain activity
35	LM of P2: pulse 1	brain activity
36	LM of P2: pulse 2, 10ms IPI	brain activity
37	LM of P2: pulse 2, 40ms IPI	brain activity
38	LM of P2: trial number	brain activity
39	LM of P2: detection	brain activity
40	LM of P2: detection x trial number	brain activity
41	mean P2: all stimuli	brain activity
42	mean P2: single-pulse	brain activity
43	mean P2: double-pulse, 10ms IPI	brain activity
44	mean P2: double-pulse, 40ms IPI	brain activity
45	standard deviation P2: all stimuli	brain activity
46	standard deviation P2: single-pulse	brain activity
47	standard deviation P2: double-pulse, 10ms IPI	brain activity
48	standard deviation P2: double-pulse, 40ms IPI	brain activity
49	latency P2: all stimuli	brain activity
50	latency P2: single-pulse	brain activity
51	latency P2: double-pulse, 10ms IPI	brain activity
52	latency P2: double-pulse, 40ms IPI	brain activity

F. Naïve Bayes Classifier

Before processing and classification, the DMp group was upsampled to achieve class balance. Minimum redundancy maximum relevance (MRMR) feature selection based on the F-test correlation quotient was used to select the single best feature and a subset of 8 features [8]. A Gaussian Naïve Bayes classifier was fit to the single best feature and to the subset of 8 features using the 'Scikit-learn' toolbox in Python. Naïve Bayes is optimal provided that the features used for classification are relatively independent, or if dependencies cancel each other out [9], which in this case is enhanced by the MRMR feature selection. Individual scores and classification performance were computed based on between subject leave-one-out cross-validation (i.e., also leaving out any corresponding samples generated by upsampling). The average ROC curve and area under the curve (AUC) were computed using between subject 10-fold cross-validation. A threshold of 0.5 balanced the sensitivity and specificity errors.

III. Results

A. Psychophysical and EEG Features

MRMR feature selection selected the psychometric slope for single-pulse stimuli as the most relevant feature. The selected subset of 8 features also included the detection threshold for single-pulse stimuli, standard deviation of the P2 component, standard deviation of the response time, psychometric slope for both types of double-pulse stimuli, and the effect of stimulus amplitude and trial number on the stimulus detection probability (obtained through logistic regression). Combination of these features in a spider plot (Fig. 2) illustrates that each condition (healthy/HC, diabetic/DM and diabetic polyneuropathy/DMp) has a characteristic fingerprint of feature values which might be used for identification of small-fiber neuropathy.

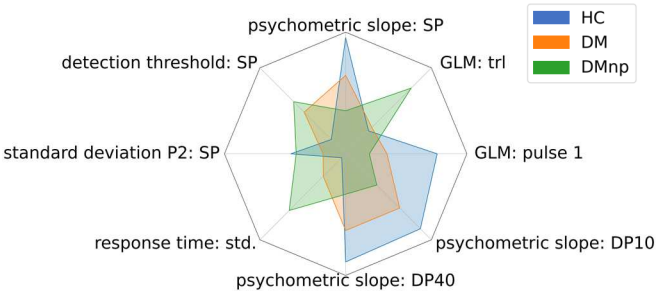

Figure 2. Spider plot including the 8 most relevant features selected through MRMR feature selection. Each condition (healthy/HC, diabetic/DM and diabetic polyneuropathy/DMp) has a characteristic fingerprint which might be used for identification of small-fiber neuropathy.

B. Naïve Bayes Classification

Assessment of the naïve bayes classification performance using leave-one-out cross-validation shows an overall accuracy of 0.70, a sensitivity of 0.57, and a specificity of 0.84 (Table II) when using the single best feature selected using MRMR. The performance significantly improved when using a combination of the 8 best psychophysical and EEG features with an accuracy of 0.87, a sensitivity of 0.92, and a specificity of 0.82. An overview of the probability of having small-fiber neuropathy assigned to each participant by the classifier during leave-one-out cross-validation, i.e., the 'neuropathy score', is shown in Fig. 3 and 4. In Fig. 3, only the single best feature is used for predicting the neuropathy score, and therefore there is a large overlap between each group. In Fig. 4, combination of the 8 best features leads to clear separation of each group, with the exception of a relatively large group of diabetic patients without diagnosed neuropathy, that were assigned to the diabetic neuropathy group. The receiver operating characteristic (ROC) and its standard deviation of the one-feature and 8-feature classifier, computed using 5-fold cross-validation, are shown in Fig. 5 and 6. The one-feature classifier shows a ROC with an area under the curve (AUC) of 0.89 +- 0.06, and the 8-feature classifier shows a ROC with a slightly larger area under the curve (AUC) of 0.92 +- 0.07.

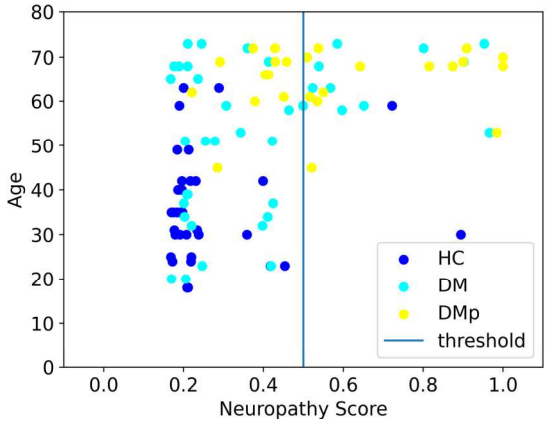

Figure 3. The probability of having small-fiber neuropathy assigned to each participant by the one-feature classifier during leave-one-out cross-validation, i.e. the 'neuropathy score'.

TABLE II. PERFORMANCE OF CLASSIFYING DIABETIC SMALL-FIBER NEUROPATHY USING THE SINGLE BEST (MRMR-1) AND THE 8 BEST (MRMR-8) FEATURES SELECTED USING MRMR. THE LARGEST VALUE OF EACH METRIC IS HIGHLIGHTED IN **BOLD**.

	Features	
	MRMR-1	***MRMR-8***
Accuracy	0.70	**0.87**
Sensitivity	0.57	**0.92**
Specificity	**0.84**	0.82

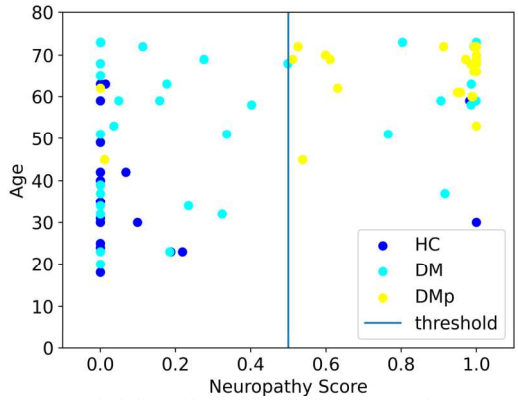

Figure 4. The probability of having small-fiber neuropathy assigned to each participant by the 8-feature classifier during leave-one-out cross-validation, i.e. the 'neuropathy score'.

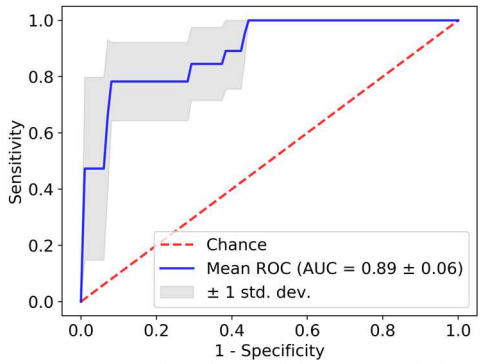

Figure 5. Receiver operating characteristic (ROC) of the one-feature classifier, computed using 5-fold cross-validation.

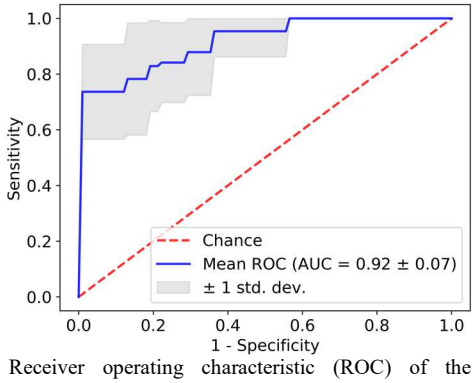

Figure 6. Receiver operating characteristic (ROC) of the 8-feature classifier, computed using 5-fold cross-validation.

IV. DISCUSSION

In this work, we used the recently developed NDT-EP method to extract individual psychophysical and EEG features from diabetes mellitus patients with and without small-fiber neuropathy, and healthy controls. We explored whether using a single feature or a selection of these features could aid identification of small-fiber neuropathy through naïve bayes classification.

Multiple features were combined to predict diabetic small-fiber neuropathy based on a naïve Bayes classifier. Whereas using only the single most significant feature resulted in an accuracy of 70.0% and an AUC of 0.89, using a larger set of 8 psychophysical and EEG features resulted in an accuracy of 87.0% and an AUC of 0.92. In both cases, the classification accuracy and AUC are able to match the accuracy and AUC of other state-of-the-art methods for the detection of small-fiber neuropathy [10]. In addition, the results show that using a combination of psychophysical and electrophysiological features can boost performance to levels that might even outperform current state-of-the-art methods. In the current results, neuropathy patients, patients with diabetes mellitus and healthy controls were not age matched, and as such classifier performance might be confounded by a difference in age between the groups. Nevertheless, scatter plots do not show any visual correlation between age and neuropathy score in the healthy and diabetes mellitus group. Further research should investigate the generalizability of this approach to other and more diverse patient groups with matched controls.

V. CONCLUSION

Using electrophysiological and psychophysical responses to intra-epidermal electrical stimulation for the identification of small-fiber neuropathy could match or even outperform current state-of-the-art methods for the diagnosis of small-fiber neuropathy. Future studies should consider this approach for the development of new diagnostic tools for small-fiber neuropathy.

REFERENCES

[1] Terkelsen, A.J., Karlsson, P, Lauria, G., Freeman, R., Finnerup, N.B., and Jensen, T.S., "The diagnostic challenge of small fibre neuropathy: clinical presentations, evaluations, and causes,", *The Lancet. Neurology,* vol. 16, no. 11, pp. 934-944, 2017.

[2] Fabry, V., et al., "Which Method for Diagnosing Small Fiber Neuropathy?", *Frontiers in Neurology*, vol. 11, no. 342, 2020.

[3] Nawroth, P.P., et al., "The Quest for more Research on Painful Diabetic Neuropathy," *Neuroscience*, vol. 387, pp. 28-37, 2018.

[4] Van den Berg, B., Doll, R.J., Mentink, A.L.H., P. Siebenga, P.S., Groeneveld, G.J., and Buitenweg, J.R., "Simultaneous tracking of psychophysical detection thresholds and evoked potentials to study nociceptive processing," *Behavior Research Methods*, 2020.

[5] Van den Berg, B., and Buitenweg, J.R., "Observation of Nociceptive Processing: Effect of Intra-Epidermal Electric Stimulus Properties on Detection Probability and Evoked Potentials," *Brain Topography*, 34(2), 139–153, 2021.

[6] Van den Berg, B., et al., "Simultaneous measurement of intra-epidermal electric detection thresholds and evoked potentials for observation of nociceptive processing following sleep deprivation" *Experimental Brain Research*, 2022, 240(2), 631–649.

[7] Doll, R.J., Veltink, P.H., and Buitenweg, J.R., "Observation of time-dependent psychophysical functions and accounting for threshold drifts," *Attention, Perception, & Psychophysics*, vol. 77, no. 4, pp. 1440-1447, 2015.

[8] Zhao, Z., Anand, R., and Wang, M., "Maximum Relevance and Minimum Redundancy Feature Selection Methods for a Marketing Machine Learning Platform," in 2019 IEEE International Conference on Data Science and Advanced Analytics (DSAA), 2019, pp. 442-452.

[9] Zhang, H., "The Optimality of Naive Bayes" in FLAIRS2004 conference, 2004.

[10] Raasing, L.R.M., Vogels, O.J.M., Veltkamp, M., Van Swol, C.F.P., and Grutters, J.C., "Current View of Diagnosing Small Fiber Neuropathy," Journal of Neuromuscular Diseases, vol. 8, pp. 185-207, 2021.